Environmental Science and Ecotechnology 20 (2024) 100410

Contents lists available at ScienceDirect

Environmental Science and Ecotechnology

journal homepage: www.journals.elsevier.com/environmental-science-and-ecotechnology/

Original Research

Electrical stress and acid orange 7 synergistically clear the blockage of electron flow in the methanogenesis of low-strength wastewater

Ze-Chong Guo [a, b, f, 1], Min-Hua Cui [c, 1], Chun-Xue Yang [e], Hong-Liang Dai [a], Tong-Yi Yang [a], Lin-Zhi Zhai [a], Yong Chen [f], Wen-Zong Liu [b, d, *], Ai-Jie Wang [b, d]

[a] School of Environmental and Chemical Engineering, Jiangsu University of Science and Technology, Zhenjiang, 212100, China
[b] State Key Laboratory of Urban Water Resource and Environment, School of Environment, Harbin Institute of Technology, Harbin, 150090, China
[c] Jiangsu Key Laboratory of Anaerobic Biotechnology, Jiangnan University, Wuxi, 214122, China
[d] School of Civil and Environmental Engineering, Harbin Institute of Technology, Shenzhen, 518055, China
[e] School of Geography and Tourism, Harbin University, Harbin, 150001, China
[f] School of Environmental Science and Engineering, Huazhong University of Science and Technology, Wuhan, 430074, China

ARTICLE INFO

Article history:
Received 7 September 2023
Received in revised form
4 March 2024
Accepted 5 March 2024

Keywords:
Methanogenesis
Conductive carrier
Electrical stress
Acid orange 7
Electron transfer

ABSTRACT

Energy recovery from low-strength wastewater through anaerobic methanogenesis is constrained by limited substrate availability. The development of efficient methanogenic communities is critical but challenging. Here we develop a strategy to acclimate methanogenic communities using conductive carrier (CC), electrical stress (ES), and Acid Orange 7 (AO7) in a modified biofilter. The synergistic integration of CC, ES, and AO7 precipitated a remarkable 72-fold surge in methane production rate compared to the baseline. This increase was attributed to an altered methanogenic community function, independent of the continuous presence of AO7 and ES. AO7 acted as an external electron acceptor, accelerating acetogenesis from fermentation intermediates, restructuring the bacterial community, and enriching electroactive bacteria (EAB). Meanwhile, CC and ES orchestrated the assembly of the archaeal community and promoted electrotrophic methanogens, enhancing acetotrophic methanogenesis electron flow via a mechanism distinct from direct electrochemical interactions. The collective application of CC, ES, and AO7 effectively mitigated electron flow impediments in low-strength wastewater methanogenesis, achieving an additional 34% electron recovery from the substrate. This study proposes a new method of amending anaerobic digestion systems with conductive materials to advance wastewater treatment, sustainability, and energy self-sufficiency.

© 2024 The Authors. Published by Elsevier B.V. on behalf of Chinese Society for Environmental Sciences, Harbin Institute of Technology, Chinese Research Academy of Environmental Sciences. This is an open access article under the CC BY-NC-ND license (http://creativecommons.org/licenses/by-nc-nd/4.0/).

1. Introduction

The objectives of wastewater treatment have evolved beyond environmental pollution control to include resource and energy recovery, driven by the global energy crisis and climate change concerns [1,2]. While anaerobic methanogenesis is a preferred method for harnessing the energy potential of wastewater, its engineering in the treatment of low-strength wastewater, characterized by a chemical oxygen demand (COD) of less than 1000 mg L^{-1}, has always been challenged by insufficient productivity and high process sensitivity [3]. Anaerobic digestion (AD) typically encompasses four stages: hydrolysis, fermentation, acetogenesis, and methanogenesis. Achieving high biogas productivity necessitates the formation of efficient methanogenic communities with unobstructed electron transfer pathways. However, under low-strength conditions, electron flow during AD, especially in acetogenesis and methanogenesis, is often impeded by the kinetic limitation of low substrate levels [4]. The metabolism rate of acetoclastic methanogens (AM) is generally very low, approximately a quarter of that of fermentative bacteria (FB), and further decreases when acetate is insufficient (with a half-saturation rate constant of 150 mg L^{-1} for AM) [5]. Additionally, in the absence of an adequate population of methanogens as hydrogen scavengers, the anaerobic oxidation of fermentation intermediates (mainly volatile fatty acids) to acetate

* Corresponding author. State Key Laboratory of Urban Water Resource and Environment, School of Environment, Harbin Institute of Technology, Harbin, 150090, China.
E-mail address: liuwenzong@hit.edu.cn (W.-Z. Liu).
[1] These authors contribute equally.

https://doi.org/10.1016/j.ese.2024.100410
2666-4984/© 2024 The Authors. Published by Elsevier B.V. on behalf of Chinese Society for Environmental Sciences, Harbin Institute of Technology, Chinese Research Academy of Environmental Sciences. This is an open access article under the CC BY-NC-ND license (http://creativecommons.org/licenses/by-nc-nd/4.0/).

Nomenclature

AO7	Acid orange 7
AM	Acetotrophic methanogens
AN	1-amino-2-naphthol
CM	Conductive materials
DIET	Direct interspecies electron transfer
EAB	Electroactive bacteria
FB	Fermentative bacteria
HPA	Hydrogen-producing acetogens
NC	Nonconductive carriers
PCR	Polymerase chain reaction
SHE	Standard hydrogen electrode
AD	Anaerobic digestion
AMA	Apparent methanogenic activity
CC	Conductive carriers
COD	Chemical oxygen demand
DNA	Deoxyribonucleic acid
ES	Electrical stress
HM	Hydrogenotrophic methanogens
HRT	Hydraulic retention time
OLR	Organic load rate
SA	Sulfanilic acid

(i.e., acetogenesis) becomes thermodynamically unfavorable [6,7]. This results in the trapping of electrons in fermentation products and exacerbates the starvation of methanogens. Therefore, it is imperative to enhance energy recovery from low-strength wastewater by employing appropriate technical means to regulate community development and overcome blockages in the electron transfer pathway during acetogenesis and methanogenesis.

Historically, methods for directly regulating the growth and metabolism of methanogens have been somewhat limited. However, a recent breakthrough has revealed that the introduction of conductive materials (CM) into AD can expedite methanogenesis by inducing a direct interspecies electron transfer (DIET) access between electroactive methanogens and electroactive bacteria (EAB) [8–10], which is faster than interspecies electron exchange via diffusive electron carriers (such as H_2 and formate) [11,12]. CM amendment enriches methanogens, accelerates system startup, and promotes systemic efficiency and stability [13–15].

In most cases, CMs were introduced into AD by dosing particle materials, but this approach faced practical challenges such as high dosage and loss, difficult separation, and potential environmental risks [11]. Given the substantial capacity and rapid processing characteristic of low-strength wastewater treatment [16], employing fixed conductive carriers (CC), whose enhancing effects have also been confirmed [17,18], is more economically and operationally feasible than dosing particle materials [11]. Furthermore, drawing from the experiences in bioelectrochemical systems, the application of electrical stress (ES) based on conductive carriers, which here also serve as electrodes, can be beneficial to methanogenesis by supplying additional electrons or habitats with suitable redox potential [19–21].

A widely overlooked issue is that a well-developed EAB population is necessary (but insufficient) to intensify DIET-type methanogenesis [22]. Currently, efforts in promoting methanogenesis through regulating EAB metabolism are limited. EAB are phylogenetically diverse and functionally versatile (such as electricity generation, metal ion or organic pollutant reduction, etc.), and they are characterized by the ability of extracellular electron transfer through cytochromes, conductive pili, or redox-active shuttles [19,23]. Interestingly, observations from studies on pollutant remediation indicated that EAB could be easily enriched in systems with exogenous electrophiles serving as electron acceptors, such as sulfate [7], nitrate [24], ferric iron [25], and even certain organic pollutants [26,27]. This presents an opportunity to enhance EAB development and metabolism by using exogenous electron acceptors as a special domestication method. Furthermore, the role of electron acceptors in promoting the degradation of organic acids has been confirmed by recent studies [28–31], which potentially alleviates the blockage in acetogenesis in low-strength environments. Acid orange 7 (AO7) is a typical azo dye with electrophilic azo bond [32] and low toxicity to methanogenesis [33], and it has been reported to effectively accelerate the decomposition of volatile organic acids (especially propionate) [29]. Therefore, it was employed in this study as a model electron acceptor, aiming to enrich EAB and accelerate acetogenesis.

This study proposed a novel strategy combining CC, ES, and AO7 to enhance methanogenesis in low-strength wastewater. Six modified anaerobic biofilters (as simplified pattern biofilm systems) treating artificial wastewater (COD ~350 mg L^{-1}) were started up under different conditions (with nonconductive or conductive carriers, with or without ES, with or without AO7). The efficacy of this strategy was assessed by evaluating methanogenic performance in the presence of ES/AO7 and subsequent removal of these factors start-up. The mechanism influencing community assembly and electron transfer was disclosed by bacterial and archaeal sequencing, electron flux balance analysis, and thermodynamic analysis. The findings contribute to an expanded understanding of electrical communication within the AD community and hold valuable insights for improving low-strength wastewater treatment processes.

2. Materials and methods

2.1. Reactor start-up and operation

Six modified up-flow anaerobic biofilters were conducted (configuration in Fig. S1 and operation scheme in Table S1), with one test group R6 (applied CC, ES, and AO7), and five distinct controls, including the conventional AD control with nonconductive carriers (NC) (R1), NC with AO7 (R2), CC alone (R3), CC with AO7 (R4), and CC with ES (R5). Each biofilter has a liquid volume of 1 L, and the filter bed was vertically divided into four equal sections (I, II, III, and IV) by perforated plates. R1 and R2 were filled with nonconductive quartz sand (resistivity >100 Ω m), while the remaining biofilters utilized conductive granular graphite (resistivity $<2 \times 10^{-6}$ Ω m), as described in Table S2. In groups with ES, sections I and III served as cathodes, and sections II and IV acted as anodes. Electrodes were contacted with a DC power supply, and a low voltage of 0.5 V was applied.

Before formal operation, reactors with ES (R5 and R6) underwent a batch mode start-up to establish electrochemical functions. Considering the influence of this stage on microbial community development, other reactors without ES (R1–R4) were also operated similarly. Specifically, all reactors were inoculated with a mixture of 100 mL effluent from a long-term operated single chamber MEC and 900 mL culture solution. This culture solution contained sodium acetate (1000 mg L^{-1}), a 50 mmol phosphate buffer solution (PBS), and trace elements [34]. The culture solution was refreshed every two days until stable current outputs were

obtained and anode potentials dropped below −400 mV (vs. Standard hydrogen electrode, SHE), indicating successful electrode acclimation.

Subsequently, all reactors transitioned to continuous mode operation under a hydraulic retention time (HRT) of 8 h, fed by artificial wastewater, consisting of glucose (given a COD of 350 mg L^{-1}), 50 mM PBS, and trace elements. AO7 was added to the influent of R2, R4, and R6 at a concentration of 50 mg L^{-1}. When methanogenic performances reached a relatively steady state after an initial lag time and fluctuation, more than ten valid running data (over 30 HRTs) were collected, and the average efficacy was calculated. The variation curve of the methane production rate and the valid data range are shown in Fig. S2. Subsequently, reactors were conducted under an HRT of 6 h for another 80 HRTs, and more than ten running data were selected and calculated similarly. The operation was at room temperature (27 ± 2 °C).

2.2. Analytics

AO7 (analytical reagent, purity >95%) was purchased from Sangon Biotech (Shanghai, China), and its concentration was quantified by an ultraviolet−visible (UV/Vis) spectrophotometer (UV-1800, Shanghai Meipuda instrument, China) at a wavelength of 484 nm. Sulfanilic acid (SA), one reduction product of AO7, was quantitatively measured with a high-performance liquid chromatography (HPLC, e2695, Waters, USA) equipped with a UV/Vis detector and a C18 column (5 μm; 4.6 × 250 mm, Symmetry, Waters, USA). COD was determined according to the standard methods (Potassium Dichromate Method). Volatile fatty acids were measured by a gas chromatography (Agilent 7890, USA). Biogas composition was analyzed by a gas chromatograph (7890A, Agilent, USA) equipped with a flame ionization and thermal conductivity detector. The current and electrode potentials were measured using a multimeter/data acquisition system (Keithley Instruments, 2700, USA).

2.3. Control tests removing ES and AO7

Control tests removing AO7 and ES were carried out after the regular operation in each HRT phase for 10 HRTs. Specifically, for R2, R4, and R6, the influent without AO7 was supplied, and the voltages in R5 and R6 were cut down. Liquid and gas samples were collected and analyzed using the same methods employed during regular operation. This control test aimed to assess the direct contribution of ES and AO7 on methanogenic performance.

2.4. Biomass sampling and analysis

Following the operation's completion, all carriers from each reactor were carefully removed and subjected to thorough washing with sterilized water, repeated 8−10 times to ensure complete detachment of the biofilm. All liquid was combined and concentrated by centrifugation (8000 rpm). The supernatant was discarded, and the residue was evenly divided into 20 samples, which were then preserved at −20 °C for subsequent biomass and metagenomics analysis.

Total biomass was assessed using three indicators: wet weight (weight after centrifugation), dry weight (dried to a constant weight at 105 °C), and total protein content, which was measured with a BCA protein assay kit (Shanghai Sangon Biotech, China) after pretreatment by an ultrasonic homogenizer (BioSafer, China). All measurements were conducted in triplicate for accuracy.

Total genomic deoxyribonucleic acid (DNA) extraction, polymerase chain reaction (PCR) amplification, bacterial 16S rDNA sequencing, archaeal 16S rDNA sequencing, and archaeal quantitative real-time PCR were all conducted by Sangon Biotech (Shanghai) Co., Ltd. Total genomic DNA of biomass sample was extracted with E. Z.N.A. Soil DNA Isolation Kit. The quantity and quality of the extracted DNA were assessed by agarose gel test. The bacterial V3−V4 region of the 16S rDNA gene was amplified using general primers Nobar_341F (CCTACGGGNGGCWGCAG) and Nobar_805R (GACTACHVGGG TATCTAATCC). Archaeal V3−V4 region of 16S rDNA was amplified using general primers 340F (CCCTAYGGGGYGCASCAG) and 1000R (GGCCATGCACYW CYTCTC) for first round amplification, 349F (GYGCASCAG KCGMGAAW) and 806R (GGACTACVSGGG TATCTAAT) for the second-round amplification. PCR products of both bacterial and archaeal amplification were purified and sent to the Illumina Miseq™ sequencing platform. Quantitative real-time PCR was performed on ABI Stepone plus PCR System with primers of 349F and 806R to quantify the total archaea in each reactor. A calibration curve (log DNA concentration versus an arbitrarily set cycle threshold value) was constructed using genomic DNA from standard plasmids. Amplification efficiency and correlation coefficients for standard curves were 81% and 0.998, respectively.

2.5. Calculations

Electrochemical efficiency was calculated according to the literature [34]. The significance of the results was determined using analyses of variance (ANOVAs) at a significance level of 0.05. Electron fluxes in three stages (fermentation, acetogenesis, and methanogenesis) in R1 and R6 were estimated based on the COD balance of all components. Both gaseous and dissolved methane were considered in the calculation. Given the absence of detectable gaseous hydrogen, it was assumed that all hydrogen converted to methane. The proportions of fermentation products were derived from literature [35], with acetate at 44%, hydrogen at 9%, and other fermentation intermediates at 47%.

Reduction potentials were calculated under specific conditions: pH = 7.0, T = 298 K, $p(H_2)$ = 5 hPa, [Acetate] = 0.05 mol L^{-1}, [Butyrate] = [Propionate] = [Ethanol] = 0.01 mol L^{-1}, [Lactate] = 0.005 mol L^{-1}, $[HCO_3^-]$ = 0.02 mol L^{-1}. The standard reduction potential of AO7 was inferred based on the fact that it can be reduced by the redox mediator anthraquinone sulphonate (AQS) (E_0' = −0.22 V) [36,37]. Note that relevant potential differences are presented as minimum values rather than exact values.

3. Results and discussion

3.1. Methanogenic performance

Reactors started up under different conditions exhibited notably distinct methanogenic efficiencies (Fig. 1). With the organic loading rate (OLR) increasing from 1.2 to 1.6 kg COD m^{-3} d^{-1} (correspondingly HRT from 8 to 6 h), the methane yield of each group significantly improved, indicating that methanogenesis was constrained by the low substrate level. This suppression was most pronounced in traditional AD (R1), with a methane production rate of less than 0.002 m^3 m^{-3} d^{-1} and a methane yield of less than 3.1 mL per g COD.

All three environmental factors (CC, ES, and AO7) demonstrated a certain promoting effect on methanogenesis ($P < 0.05$). Specifically, compared to R1, AO7 alone (R2) led to a 2−3-fold increase in methanogenic productivity, while CC (R3) resulted in a 14.7−27.1-fold promotion under an HRT of 6 h. For the systems with CC, applying ES (R5) further slightly accelerated methanogenesis with up to a 33.0-fold increase compared to R1, while AO7 (R4) produced contradictory effects under two hydraulic conditions.

Remarkably, the simultaneous application of CC, AO7, and ES

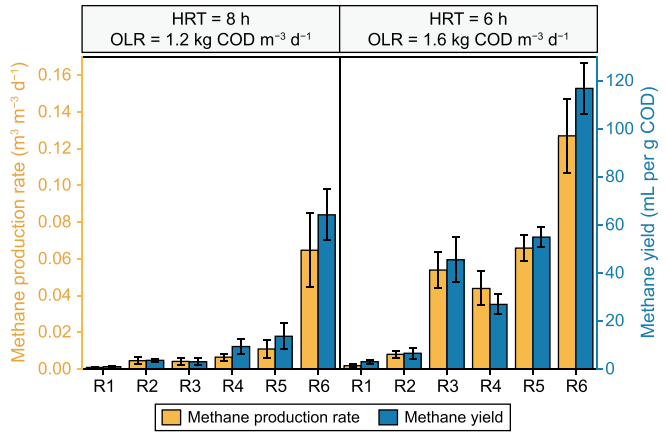

Fig. 1. Average methane production rate and yield under a hydraulic retention time (HRT) of 8 and 6 h.

(R6) caused a substantial boost in methanogenesis, surpassing the cumulative effects of each factor. Under an HRT of 8 h, the methane production rate and methane yield of R6 were 0.065 m^3 m^{-3} d^{-1} and 64.3 mL per g COD, respectively, 63.5 and 72.0 times higher than those of R1. These indexes increased to 0.127 m^3 m^{-3} d^{-1} and 116.9 mL per g COD under an HRT of 6 h. This outstanding enhancement highlights the synergistic stimulating effect of three factors on methanogenesis.

In this study, to elucidate the regulatory role of CC, ES, and AO7, only extremely low biomass (less than 1% of the final biomass) was initially inoculated into the system. Biofilms proliferated and colonized spontaneously under unfavorable conditions, including constant low strength, high-rate operation, and non-optimal temperature. In addition, dissolved methane was not counted, which is estimated to account for approximately 40% of the total methane, according to Henry's law [38]. Despite the suboptimal overall performance due to these constraints, the current results fully demonstrate the effectiveness of the reinforcement strategy. This insight is enlightening for upgrading various biofilm-based methanogenic engineering of low-strength wastewater.

3.2. Performance without ES & AO7

To discern the direct contribution of ES and AO7 to methanogenesis, control tests removing ES and AO7 after regular operation were performed (Fig. 2). Without ES and AO7, the decline in methanogenic performance in each group was minimal or even insignificant (Table S3). This suggests that, after sufficient domestication, the methanogenic performance became independent of the continuous supply of ES and AO7. This implies that the effect of ES and AO7 was attributed to the enhancement of biofilms' metabolic function rather than direct contributions to methanogenesis.

Despite the remarkable promoting effect, adding AO7 (typically considered an organic pollutant) presented a potential risk of secondary pollution. Encouragingly, the results suggest that ES and AO7 can only be applied temporarily during the startup or adjustment phases. This reduces the safety risk associated with AO7 use, making the strengthening strategy more practical and economically feasible.

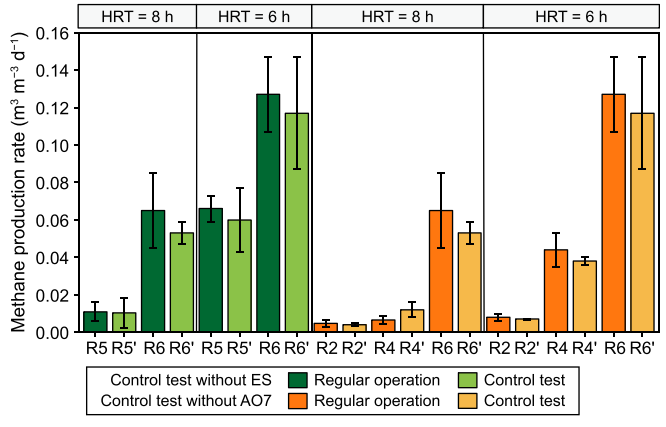

Fig. 2. Methanogenic efficiency in control tests removing electrical stress (ES) and acid orange 7 (AO7). R stands for regular operation, R′ stands for control tests without ES and AO7.

3.3. Methanogenic activity and archaeal content of biomass

The biomass activity in the AD system is generally evaluated by specific methanogenic activity tests. However, considering the mediation of CC, the isolated biofilms' methanogenic activity may not accurately represent their *in situ* state. Therefore, in this experiment, an apparent methanogenic activity (AMA) was calculated based on the total biomass in the bioreactor and the *in situ* methanogenic performance in control tests without ES and AO7 (Table 1). The total biomass was promoted by CC ($P < 0.05$), likely attributed to its surface properties. ES did not significantly affect total biomass ($P > 0.05$). AO7, however, reduced the wet and dry weight of total biomass ($P < 0.05$) but did not impact protein amount ($P > 0.05$). This discrepancy may be due to AO7's influence on forming or degrading intracellular reserve polymers, such as glycogen and trehalose, commonly found in sugar-fed dynamic AD systems [39].

All factors (CC, ES, and AO7) positively influenced AMA, with R6 showcasing superior performance compared to other controls. The archaeal content in unit biomass mirrored the same trend (Table 1) and exhibited a positive linear correlation with AMA (Fig. S3). According to the archaeal sequencing results, over 90% of archaea were identified as methanogens. Consequently, the archaeal content in biomass can be approximated as the content of methanogens. Both AMA and archaeal content directly demonstrate that, under the mediation of CC, the synergistic application of ES and AO7 significantly promoted the proliferation of methanogens and enhanced the methanogenic function of the microbial community.

3.4. Electron flux analysis

Based on the COD balance of all components, electron fluxes in three stages (fermentation, acetogenesis, and methanogenesis) were estimated for both R1 (conventional AD) and R6 (with ES and AO7 removed) (Fig. 3a and b). Inevitably, a significant portion of electrons (40–60%) was consumed for microbial growth and stored as intracellular reserve polymers. The insufficient decomposition of reserve polymers under short HRTs led to some wastage of electrons, while ES and AO7 can alleviate this problem.

In a conventional AD system (R1), there was almost no electron flow between metabolites after the initial electron distribution during the fermentation stage. Electrons in most fermentation products (except hydrogen) were directly lost to the effluent. This indicates that only fermentative biochemical reactions were sufficient, but the electronic pathways of subsequent acetogenesis and acetotrophic methanogenesis were severely obstructed, and the metabolic functions of related microbial populations were not fully realized.

In R6, electrons originating from fermentation intermediates to acetate and hydrogen increased from 1% to 19%, and a substantial

Table 1
Total biomass, apparent methanogenic activity (AMA), and archaeal content in the biofilm of each group.

Group	Total biomass (g)			Daily methane production[a] ($L\ d^{-1}$)	Apparent methanogenic activity[c] (L_{CH_4} per d per g biomass)	Archaeal content[d] (copies per g biomass)
	Wet weight	Dry weight	Protein			
R1	12.09 ± 0.18	2.07 ± 0.52	0.07 ± 0.01	0.002	0.03	1.6×10^5
R2	10.33 ± 0.18	2.50 ± 0.06	0.08 ± 0.01	0.007[b]	0.09	2.1×10^5
R3	25.11 ± 0.15	7.14 ± 0.13	0.18 ± 0.02	0.054	0.30	3.6×10^5
R4	10.85 ± 0.41	1.19 ± 0.28	0.12 ± 0.01	0.038[b]	0.32	3.7×10^5
R5	24.57 ± 1.30	6.34 ± 0.77	0.17 ± 0.02	0.059[b]	0.35	4.7×10^5
R6	10.99 ± 0.39	1.41 ± 0.06	0.16 ± 0.02	0.117[b]	0.73	7.1×10^5

[a] Average methane production (dissolved methane not included) under an HRT of 6 h.
[b] Data in control tests without ES and AO7.
[c] Total protein amount used as total biomass in the calculation.
[d] Analyzed by real-time qPCR with general archaeal prime.

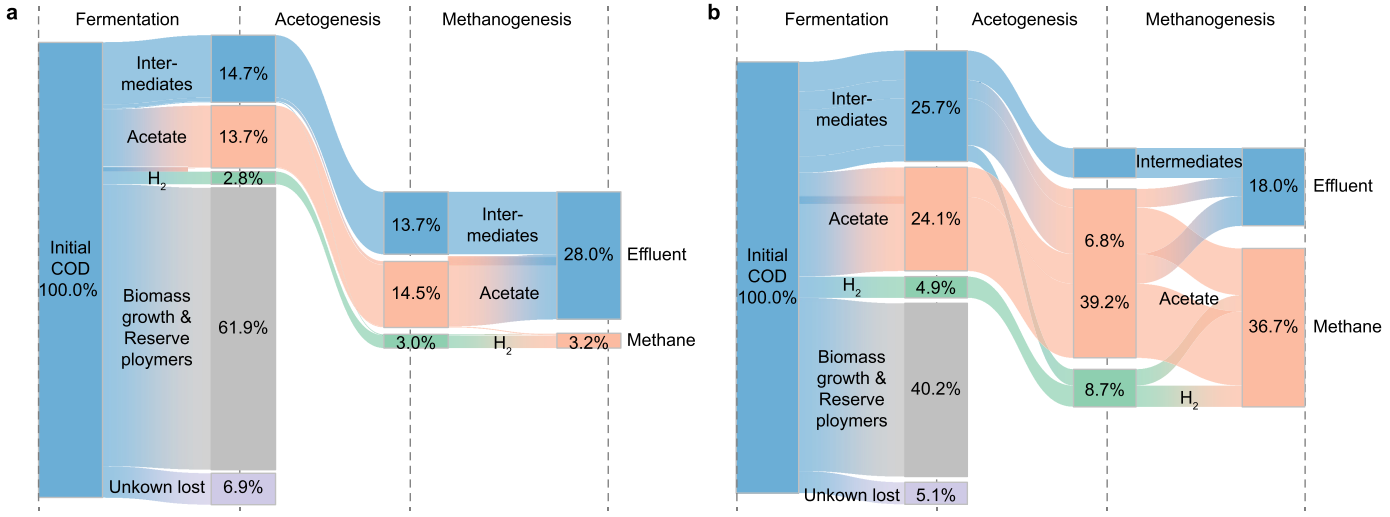

Fig. 3. Estimated electron flux in anaerobic digestion in R1 (**a**) and R6 (**b**).

portion of electrons in acetate (71%) flowed to methane. This indicates that the modulation of CC, ES, and AO7 stimulated the electronic communication between microbial populations, scavenged the blockage of electron flow in acetogenesis and acetotrophic methanogenesis, and reduced the number of wasted electrons in reserve polymers and effluent.

3.5. Bacterial community assembly

In an AD system, the electron communication between metabolites relies on the metabolism of various microbial populations, so understanding the microbial community's structure is crucial. Given the small initial biomass (less than 1% of the final biomass) and the extended culture time (over 120 days) in this experiment, it is reasonable to assume the microbial community assembly, particularly the evolution of functional populations, was dominated by the deterministic effect of environmental factors rather than stochastic effect. The community's responses to each factor can be elucidated through statistical analysis.

Bray-Curtis analysis (Fig. 4a) highlighted a significant difference between groups without AO7 (R1, R3, and R5) and those with AO7 (R2, R4, and R6) in bacterial community structures. This indicates that AO7, rather than CC or ES, played a decisive role in bacterial community assembly. AO7 notably increased bacterial community diversity (Fig. 4b) and influenced the distribution of metabolic groups (Fig. 4c). Despite variations in genera composition (dominant genera abundance summarized in Table S4), the abundance of each metabolic population was quite similar in AO7-free (or AO7-adding) groups.

FB are fast-growing flora responsible for fermenting glucose or glycolytic products to various acids, CO_2, and H_2, mainly including lactic acid bacterium *Lactococcus* [40], acetate and propionate producer *Alkaliflexus* [41], *Propionivibrio* [42], and so on. FB was the most abundant in all groups, accounting for 74.5 ± 0.6% in groups without AO7 and 41.5 ± 2.2% in groups with AO7.

In typical AD systems, the conversion of fermentation intermediates to acetate and hydrogen mainly relies on syntrophic hydrogen-producing acetogens (HPA) [43,44]. As the symbiotic partner, HPA's evolution and metabolism are regulated by methanogenesis and are difficult to develop in low-strength wastewater [6,7]. In this experiment, only three acetogenic genera were detected with extremely low abundances (1.0 ± 0.4% without AO7 and 3.2 ± 0.3% with AO7), including two HPA (*Candidatus* Cloacamonas and *Syntrophomonas*) [45–47] and one homoacetogen (*Acetobacterium*), which produces acetate from CO_2 and H_2 [48]. The scarcity of acetogens explained the blocked electron flow during acetogenesis in R1.

AO7 significantly facilitated the enrichment of various EAB (from 7.1 ± 1.0% to 23.7 ± 3.2%). This group included genera such as *Aeromonas*, *Geobacter*, *Enterococcus*, and *Raoultella*, as well as serval sulfate-reducing bacteria (*Desulfovibrio*, *Desulfuromonas*, *Desulfitibacter*, and *Desulfobulbus*). Most genera have azoreductases, allowing them to utilize AO7 as an electron acceptor in anaerobic respiration [49–51]. Additionally, with the mediation of conductive materials, methanogens can act as electron acceptors for some EAB in DIET-type methanogenesis [12,52]. EAB are metabolically

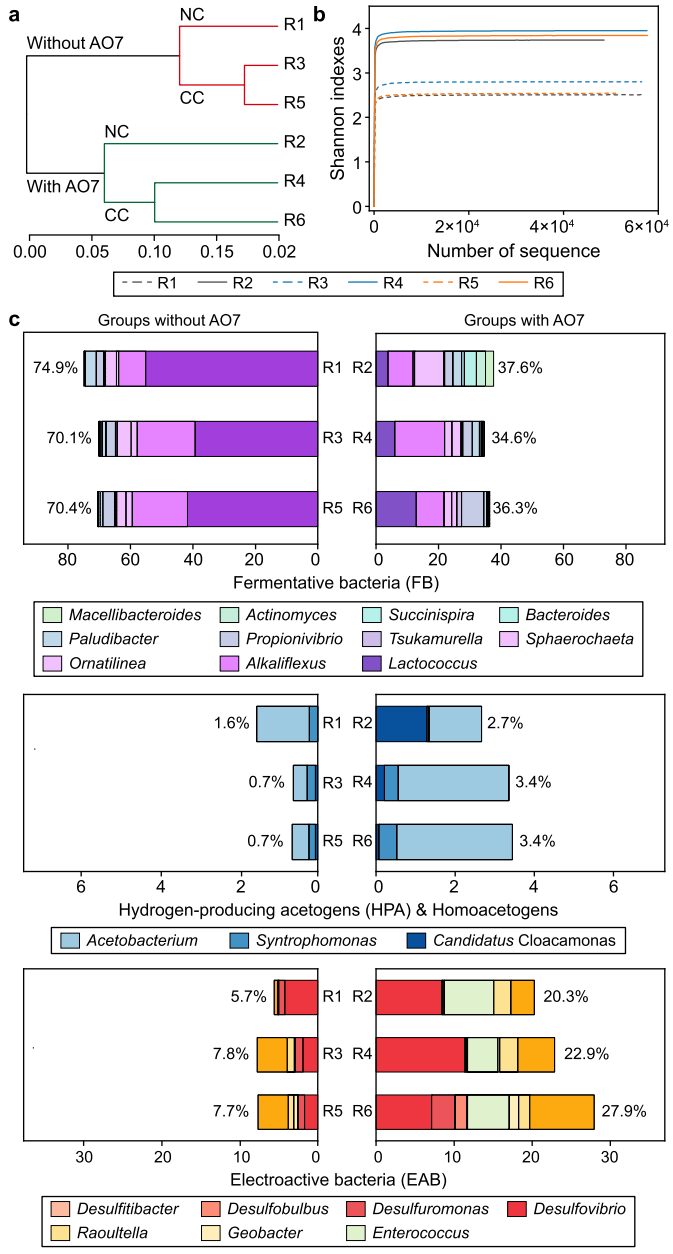

Fig. 4. **a**, Bray-Curtis analysis of bacterial community structure. **b**, Shannon rarefaction plot. **c**, Metabolic group abundance and genera distribution. NC stands for nonconductive carrier, and CC stands for conductive carrier.

versatile, utilizing a variety of intermediates as electron and energy donors, which are oxidized either completely to CO_2 or partially to smaller organic compounds [53–55].

Interestingly, it is observed that conductive materials and electrodes with low external voltage are not as effective as soluble electron acceptors (like AO7) in enriching EAB (2% vs. 15% increase). This disparity can be attributed to the challenges associated with electron transfer. Compared to the well-diffused and cell-penetrable soluble acceptors, the electron transfer between extracellular solid mediators and EAB is more difficult and generally limited by spatial distance [12,56].

Another noteworthy observation is that the enrichment of EAB does not necessarily lead to improved methanogenic efficiency, as seen in the case of R4. The ecological relationship between EAB and methanogens (whether cooperative or competitive) mainly depends on environmental factors [57]. Even under the mediation of conductive materials, DIET-type methanogenic syntrophs may not be fully established.

In general, in the absence of AO7, the bacterial community was "monopolized" by FB, while other populations faced challenges in development. In particular, the scarcity of acetogens led to a blocked electron flux during acetogenesis. The introduction of AO7 was crucial in reshaping the bacterial community, promoting diversity, and enriching EAB. This enrichment of EAB potentially contributes more electrons for methanogens, either through DIET with the mediation of CC or by facilitating the partially oxidizing intermediates to acetate.

3.6. Archaeal composition

Different from the bacterial community, according to archaeal sequencing results (Fig. 5a), the archaeal community structure was mainly determined by CC and ES rather than AO7. The genera distribution further reveals distinct patterns (Fig. 5b). In groups with NC, like R1 and R2, *Methanobrevibacter*, a hydrogenotrophic methanogen (HM) [58], dominated with a relative abundance ranging from 36.4% to 76.2%. On the other hand, groups with CC (R3 to R6) were characterized by the dominance of another HM, *Methanobacterium*, accounting for 46.1–66.1% of the community. *Methanobacterium* is known for its ability to accept electrons from electrodes or syntrophic partners [59].

In a well-functioning AD system, AM typically dominates the methanogenic community, constituting about 70% of the population. However, due to its faster growth rate, HM tends to prevail over AM in low-strength environments. In R1, the content of AM was notably low, accounting for only 1.6%. The application of ES induced a significant increase in AM content. *Methanosarcina*, a typical AM that could participate in DIET-type methanogenesis [60], was specifically enriched (4.4% in R5 and 27.2% in R6). This enrichment well explained the promoted electron flux in acetophilic methanogenesis in R6. The response of *Methanosarcina* to ES and AO7 and its important role in promoting AMA were also confirmed by canonical correlation analysis between characteristic genera, environmental factors, and AMA (Fig. S4).

3.7. The synergistic mechanism of AO7 and ES

As previously mentioned, AO7 and ES profoundly affected the microbial community's composition and function, mainly attributed to their intervention on microbial metabolism in the biofilm formation (start-up or adjustment) stage.

In anaerobic conditions, the −N=N- bond in AO7 can be biologically (in R2, R4, and R6) or electrochemically (in R6, less than

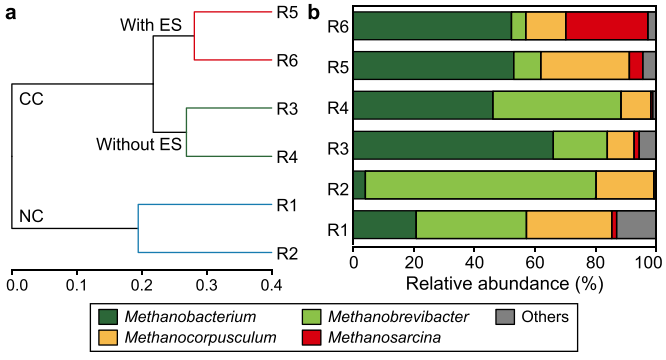

Fig. 5. **a**, Bray-Curtis analysis of archaeal community structure. **b**, Archaeal distribution at the genus level.

60% of the total reduction) reduced, resulting in the production and two reduction products, SA and 1-amino-2-naphthol (AN) (equation (1)) [33].

Considerable AO7 decolorization efficiencies ranging from 85% to 98% and high product recovery efficiencies in 84%–92% were observed in all groups (details in Table S5), suggesting a sufficient reduction of AO7. The reduction products of AO7 can be fully mineralized under aerobic conditions [61]. Therefore, the environmental risks associated with introducing AO7 can likely be mitigated by following an appropriate oxidation operation.

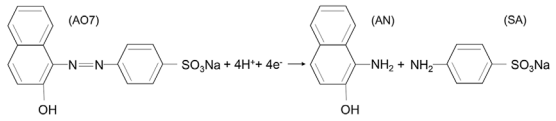

(1)

The respiration of anaerobic flora exhibits great flexibility, and various redox pairs with potential differences can generate electron flow in their respiratory chain and provide energy for their growth. In typical AD without exogenous electron acceptors, the acetogenesis of fermentation intermediates, such as lactate, butyrate, propionate, and ethanol, is generally accompanied by H^+ reduction, which is thermodynamically feasible only at very low hydrogen partial pressures. In the start-up stage, hydrogen consumers are usually lacking due to the slow growth of methanogens, especially in low-strength wastewater, leading to hydrogen inhibition on acetogenesis. This issue can be addressed by the addition of AO7.

Fig. 6a shows the reduction potentials of redox couples of some typical fermentation intermediates at a hydrogen partial pressure of 5 hPa. In the absence of AO7, only ethanol and lactate can be oxidized by H^+, while the acetogenesis of butyrate and propionate cannot be carried out. Adding AO7 increases the potential of electron acceptors in the AD system, making the oxidation of various intermediates thermodynamically feasible. The specific reactions that take place depend on the metabolic properties of the bacteria present. For instance, among the EAB detected in this study, *Desulfovibrio* mainly produces acetate, which accumulates as the end product of the oxidation of lactate, malate, pyruvate, and other organics [62]. *Desulfuromonas* generally conducts complete acetate oxidation, and some species can also use propionate and lactate [53,54]. *Desulfobulbus* can propionate oxidizing [55], and *Geobacter* prefers acetate and ethanol [12]. Importantly, using AO7 as an acceptor is advantageous in providing metabolic energy because it can increase the reaction electromotive force. Therefore, bacteria with AO7-reducing ability generally have a higher growth rate and are easier to enrich in the system. It is worth noting that the role of AO7 may not be unique, and other substances with high reduction potentials (or wastewater containing electrophilic pollutants) may have similar functions.

Beware that AO7, with a higher reduction potential than the redox couples Acetate/CH_4 and HCO_3^-/CH_4 (about −0.24 V), may compete with methanogens for acetate and hydrogen, which could explain the contradictory effects of AO7 on methanogenesis in R4. Similar issues arise with other electron acceptors like sulfate and iron ions [7]. Theoretically, whether electron acceptors competitively inhibit methanogenesis depends on various factors, such as the type of electron donors, the concentration of electron acceptors, and their degradation dynamics [63,64]. Their concentration should be carefully considered when applying exogenous electron acceptors for methanogenesis promotion. Using them as a short-term regulation rather than a continuous condition may be more beneficial.

In many cases where AD was coupled with bioelectrochemical systems, the improvement in methanogenesis is mainly attributed to the direct contribution of various electrochemical reactions, such as hydrogen evolution, methane electrosynthesis, and anode respiration [20,65]. However, in this study, the situation was quite different. Despite the current generation by ES in R5 and R6, the low electrochemical efficiency (seen in Table S6) indicates that the promoting effect obtained was not primarily due to the direct contribution of electrochemical processes. The average currents in R5 and R6 were less than 1.5 mA (corresponding to a current density of less than 1.5 A per m^3 of reactor volume), and anode coulombic efficiencies were less than 1%. Moreover, the theoretical maximum contributions of circuit current to methanogenesis (assuming all electrons in the circuit are involved in methanogenesis) were less than 3%. It suggests that the electrochemical

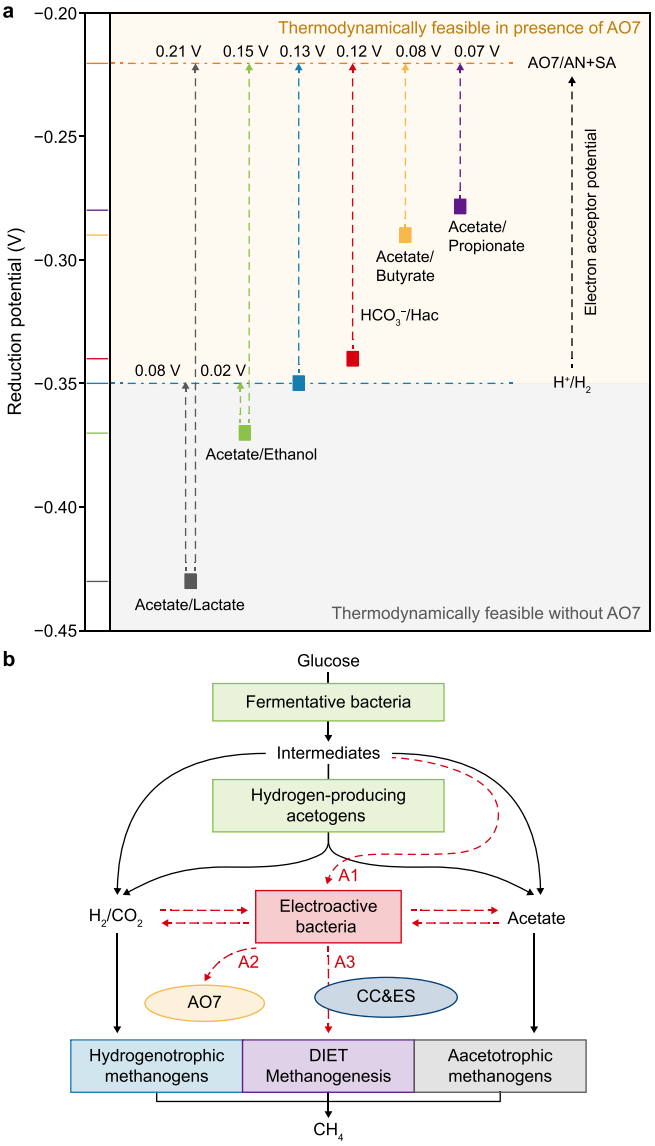

Fig. 6. **a**, The possible redox reactions and their estimated electromotive force in the system with and without acid orange 7 (AO7). **b**, Hypothetical influencing mechanism of the conductive carrier (CC), electrical stress (ES), and AO7 on anaerobic digestion metabolic network. A1: intermediates, acetate, and hydrogen oxidized by electroactive bacteria; A2: electroactive bacteria takes AO7 as an electron acceptor; A3: direct interspecies electron transfer (DIET) between electroactive bacteria and methanogens under the mediation of CC and the stimulation of ES.

process' direct contribution to organic matter degradation and methanogenesis was negligible. This observation explains why methanogenic efficiency was not significantly reduced after removing ES.

Referring to the analyses of the archaeal community and electron flux, it can be inferred that ES promoted the electron flow in acetotrophic methanogenesis in a manner that excluded the current's direct contribution. This effect was likely due to alternations in the electrochemical state of the carrier surface. Without ES, the carrier potential was about −0.25 V (vs. SHE), and with ES, the potential at the cathode was about −0.5 V (vs. SHE). The low-potential carrier surface may influence the electrochemical gradient of attached methanogens for basic cellular functions, including chemo-osmotic transport and ATP synthesis [66,67]. Alternatively, the presence of an electric field force could cause a directional guiding effect on the originally disordered electron transfer on the carrier and make it easier for methanogens to establish electrical connections with EAB.

Overall, the combination of CC, ES, and AO7 synergistically affected the assembly and metabolism of the anaerobic community in low-strength wastewater (Fig. 6b). AO7, acting as an exogenous electron acceptor, enriched EAB and promoted the degradation of organic acids. With the mediation of CC and the stimulation of ES, the electrical communication between EAB and methanogens is enhanced. This facilitated the establishment of a metabolic network involving EAB respiration and DIET methanogenesis, overcoming the blockage of electron flow and resulting in more efficient recovery of electrons from the substrate.

4. Conclusion

Simultaneously applying CC, ES, and AO7 in a biofilm system generated a synergistic effect on functional community domestication and methanogenesis. AO7 enhanced the acetogenesis of fermentation intermediates by acting as an exogenous electron acceptor and reshaped the bacterial community structure by enriching electroactive bacteria. CC and ES, in contrast, regulated the archaeal community assembly and promoted electrotrophic methanogen proliferation. The combined action of these three factors synergistically cleared the blockage in electron flow, constructing a more efficient metabolic network in low-strength wastewater methanogenesis.

CRediT authorship contribution statement

Ze-Chong Guo: Conceptualization, Investigation, Data Curation, Writing - Original Draft. **Min-Hua Cui:** Conceptualization, Methodology, Writing - Original Draft. **Chun-Xue Yang:** Methodology, Data Curation. **Hong-Liang Dai:** Formal Analysis, Writing - Review & Editing. **Tong-Yi Yang:** Writing - Review & Editing. **Lin-Zhi Zhai:** Writing - Review & Editing. **Yong Chen:** Writing - Review & Editing. **Wen-Zong Liu:** Project Administration, Writing - Review & Editing, Supervision. **Ai-Jie Wang:** Writing - Review & Editing, Supervision.

Declaration of competing interest

The authors declare that they have no known competing financial interests or personal relationships that could have appeared to influence the work reported in this paper.

Acknowledgments

This research was supported by the National Natural Science Foundation of China (No. 52000090 and No. 52370171), the National Science Foundation of China (No. 52321005), the China Postdoctoral Science Foundation (No. 2021M701511), the Shenzhen Overseas High-level Talents Research Startup Program from Harbin Institute of Technology (Shenzhen) and the Natural Science Foundation of Guangdong Province for Distinguished Young Scientists (No. 2021B1515020084).

Appendix A. Supplementary data

Supplementary data to this article can be found online at https://doi.org/10.1016/j.ese.2024.100410.

References

[1] D. Puyol, D. Batstone, T. Hulsen, S. Astals, M. Peces, J.O. Kromer, Resource recovery from wastewater by biological technologies: opportunities, challenges, and prospects, Front. Microbiol. 7 (2017) 2106.
[2] Z. Yin, L. Zhu, S. Li, T. Hu, R. Chu, F. Mo, D. Hu, C. Liu, B. Li, A comprehensive review on cultivation and harvesting of microalgae for biodiesel production: environmental pollution control and future directions, Bioresour. Technol. 301 (2020) 122804.
[3] D.J. Batstone, B. Virdis, The role of anaerobic digestion in the emerging energy economy, Curr. Opin. Biotechnol. 27 (2014) 142–149.
[4] A.J. Wang, W.W. Li, H.Q. Yu, Advances in biogas Technology, in: F.W. Bai, C.G. Liu, H. Huang, G. Tsao (Eds.), Biotechnology in China III: Biofuels and Bioenergy. Advances in Biochemical Engineering Biotechnology, Springer, Berlin, Heidelberg, Berlin, Heidelberg, 2011.
[5] R. Mo, W. Guo, D. Batstone, J. Makinia, Y. Li, Modifications to the anaerobic digestion model no. 1 (ADM1) for enhanced understanding and application of the anaerobic treatment processes – a comprehensive review, Water Res. 244 (2023) 120504.
[6] G. Baek, J. Kim, J. Kim, C. Lee, Role and potential of direct interspecies electron transfer in anaerobic digestion, Energies 11 (1) (2018) 107.
[7] W. Qiao, K. Takayanagi, Q. Li, M. Shofie, F. Gao, R. Dong, Y.Y. Li, Thermodynamically enhancing propionic acid degradation by using sulfate as an external electron acceptor in a thermophilic anaerobic membrane reactor, Water Res. 106 (2016) 320–329.
[8] T. Wang, D. Zhang, L. Dai, B. Dong, X. Dai, Magnetite triggering enhanced direct interspecies electron transfer: a scavenger for the blockage of electron transfer in anaerobic digestion of high-solids sewage sludge, Environ. Sci. Technol. 52 (12) (2018) 7160–7169.
[9] F. Liu, A.-E. Rotaru, P.M. Shrestha, N.S. Malvankar, K.P. Nevin, D.R. Lovley, Promoting direct interspecies electron transfer with activated carbon, Energy Environ. Sci. 5 (10) (2012) 8982–8989.
[10] D.R. Lovley, Syntrophy goes electric: direct interspecies electron transfer, Annu. Rev. Microbiol. 71 (1) (2017) 643.
[11] Z. Zhao, Y. Li, Y. Zhang, D.R. Lovley, Sparking anaerobic digestion: promoting direct interspecies electron transfer to enhance methane production, iScience 23 (12) (2020) 101794.
[12] D.R. Lovley, Happy together: microbial communities that hook up to swap electrons, ISME J. 11 (2) (2017) 327–336.
[13] G. Martins, A.F. Salvador, L. Pereira, M.M. Alves, Methane production and conductive materials: a critical review, Environ. Sci. Technol. 52 (18) (2018) 10241–10253.
[14] Q. Yin, G. Wu, Advances in direct interspecies electron transfer and conductive materials: electron flux, organic degradation and microbial interaction, Biotechnol. Adv. 37 (8) (2019) 107443.
[15] H. Liu, Y. Xu, L. Li, X. Dai, L. Dai, A review on application of single and composite conductive additives for anaerobic digestion: advances, challenges and prospects, Resour. Conserv. Recycl. 174 (2021) 105844.
[16] C. Wang, C. Wang, L. Jin, D. Lu, H. Chen, W. Zhu, X. Xu, L. Zhu, Response of syntrophic aggregates to the magnetite loss in continuous anaerobic bioreactor, Water Res. 164 (2019) 114925.
[17] Z. Guo, L. Gao, L. Wang, W. Liu, A. Wang, Enhanced methane recovery and exoelectrogen-methanogen evolution from low-strength wastewater in an up-flow biofilm reactor with conductive granular graphite fillers, Front. Environ. Sci. Eng. 12 (4) (2018) 131–140.
[18] J. Liu, T. Liu, S. Chen, H. Yu, Y. Zhang, X. Quan, Enhancing anaerobic digestion in anaerobic integrated floating fixed-film activated sludge (An-IFFAS) system using novel electron mediator suspended biofilm carriers, Water Res. 175 (2020) 115697.
[19] F. Kracke, I. Vassilev, J.O. Kromer, Microbial electron transport and energy conservation - the foundation for optimizing bioelectrochemical systems, Front. Microbiol. 6 (2015) 575.
[20] Z. Guo, W. Liu, C. Yang, L. Gao, S. Thangavel, L. Wang, Z. He, W. Cai, A. Wang, Computational and experimental analysis of organic degradation positively regulated by bioelectrochemistry in an anaerobic bioreactor system, Water Res. 125 (2017) 170–179.
[21] L. Wang, C. Yang, T. Sangeetha, Z. He, Z. Guo, L. Gao, A. Wang, W. Liu, Methane production in a bioelectrochemistry integrated anaerobic reactor with layered nickel foam electrodes, Bioresour. Technol. 313 (2020) 123657.
[22] S. Zhang, J. Chang, W. Liu, Y. Pan, K. Cui, X. Chen, P. Liang, X. Zhang, Q. Wu,

Y. Qiu, X. Huang, A novel bioaugmentation strategy to accelerate methanogenesis via adding *Geobacter sulfurreducens* PCA in anaerobic digestion system, Sci. Total Environ. 642 (2018) 322–326.
[23] G. Pankratova, L. Hederstedt, L. Gorton, Extracellular electron transfer features of Gram-positive bacteria, Anal. Chim. Acta 1076 (2019) 32–47.
[24] Y.Q. Lu, Y. Xu, S.S. Chen, B. Dong, X.H. Dai, Effect of nitrite addition on the two-phase anaerobic digestion of waste activated sludge: optimization of the acidogenic phase and influence mechanisms, Environ. Pollut. 261 (5) (2020) 114085.
[25] Z.W. He, C.X. Yang, C.C. Tang, W.Z. Liu, A.J. Zhou, Y.X. Ren, A.J. Wang, Response of anaerobic digestion of waste activated sludge to residual ferric ions, Bioresour. Technol. 322 (2021) 124536.
[26] Z.C. Guo, L. Zhang, M.H. Cui, A.J. Wang, Electrode microbial communities associated with electron donor source types in a bioelectrochemical system treating azo-dye wastewater, Water 14 (9) (2022) 1505.
[27] J. Li, W.T. Li, G. Luo, Y. Li, A.M. Li, Effect of nitrobenzene on the performance and bacterial community in an expanded granular sludge bed reactor treating high-sulfate organic wastewater, Front. Environ. Sci. Eng. 13 (1) (2019) 6.
[28] F. Zan, T. Hao, Sulfate in anaerobic co-digester accelerates methane production from food waste and waste activated sludge, Bioresour. Technol. 298 (2020) 122536.
[29] Y. Li, Y. Zhang, X. Quan, J. Zhang, S. Chen, S. Afzal, Enhanced anaerobic fermentation with azo dye as electron acceptor: simultaneous acceleration of organics decomposition and azo decolorization, J. Environ. Sci. (China) 26 (10) (2014) 1970–1976.
[30] C.X. Yang, L. Wang, Y.J. Zhong, Z.C. Guo, L. Jia, S.P. Yu, T. Sangeetha, B.L. Liu, C. Ni, H. Guo, Efficient methane production from waste activated sludge and Fenton-like pretreated rice straw in an integrated bio-electrochemical system, Sci. Total Environ. 813 (2022) 152411.
[31] A.J. Zhou, H.Y. Liu, C. Varrone, A. Shyryn, Z. Defemur, S.F. Wang, W.Z. Liu, X.P. Yue, New insight into waste activated sludge acetogenesis triggered by coupling sulfite/ferrate oxidation with sulfate reduction-mediated syntrophic consortia, Chem. Eng. J. 400 (2020) 125885.
[32] M.H. Cui, W.Z. Liu, D. Cui, Recent advancements in azo dye decolorization in bio-electrochemical systems (BESs): insights into decolorization mechanism and practical application, Water Res. 203 (2021) 117512.
[33] M.H. Cui, D. Cui, L. Gao, A.J. Wang, H.Y. Cheng, Azo dye decolorization in an up-flow bioelectrochemical reactor with domestic wastewater as a cost-effective yet highly efficient electron donor source, Water Res. 105 (2016) 520–526.
[34] Z. Guo, S. Thangavel, L. Wang, Z. He, W. Cai, A. Wang, W. Liu, Efficient methane production from beer wastewater in a membraneless microbial electrolysis cell with a stacked cathode: the effect of the cathode/anode ratio on bioenergy recovery, Energy Fuels 31 (1) (2016) 615–620.
[35] S.V. Kalyuzhnyi, M.A. Davlyatshina, Batch anaerobic digestion of glucose and its mathematical modeling 1 Kinetic investigations, Bioresour. Technol. 59 (1) (1997) 73–80.
[36] F.P. Van der Zee, F.J. Cervantes, Impact and application of electron shuttles on the redox (bio)transformation of contaminants: a review, Biotechnol. Adv. 27 (3) (2009) 256–277.
[37] J. Rau, H.J. Knackmuss, A. Stolz, Effects of different quinoid redox mediators on the anaerobic reduction of azo dyes by bacteria, Environ. Sci. Technol. 36 (7) (2002) 1497–1504.
[38] H. Yeo, J. An, R. Reid, B.E. Rittmann, H.S. Lee, Contribution of liquid/gas mass-transfer limitations to dissolved methane oversaturation in anaerobic treatment of dilute wastewater, Environ. Sci. Technol. 49 (17) (2015) 10366–10372.
[39] B.J. Ni, D. Batstone, B.H. Zhao, H.Q. Yu, Microbial internal storage alters the carbon transformation in dynamic anaerobic fermentation, Environ. Sci. Technol. 49 (15) (2015) 9159–9167.
[40] S.Y. Yang, Y. Zheng, Z. Huang, X.M. Wang, H. Yang, *Lactococcus nasutitermitis* sp. nov. isolated from a termite gut, Int. J. Syst. Evol. Microbiol. 66 (1) (2016) 518–522.
[41] J. Zhao, H. Zhang, D. Guan, Y. Wang, Z. Fu, Y. Sun, D. Wang, H. Zhang, New insights into mechanism of emerging pollutant polybrominated diphenyl ether inhibiting sludge dark fermentation, Bioresour. Technol. 368 (2023) 128358.
[42] C.J. Xie, R. Tang, S. Yang, S. Han, C. Rensing, G.H. Liu, S.G. Zhou, A novel nitrogen-fixing bacterium, *Propionivibrio soli* sp. nov. isolated from paddy soil, Arch. Microbiol. 205 (2) (2023) 68.
[43] S. Wang, J. Li, C. Liu, L.R. Nies, J.Z. Li, Enhanced methane production through bioaugmentation of butyrate-oxidizing hydrogen-producing acetogens in anaerobic wastewater treatment, Environ. Prog. Sustain. Energy 37 (1) (2018) 367–374.
[44] C. Huang, W. Wang, X.Y. Sun, J.Y. Shen, L.J. Wang, A novel acetogenic bacteria isolated from waste activated sludge and its potential application for enhancing anaerobic digestion performance, J. Environ. Manag. 255 (2020) 109842.
[45] N.M. Juste-Poinapen, M.S. Turner, K. Rabaey, B. Virdis, D.J. Batstone, Evaluating the potential impact of proton carriers on syntrophic propionate oxidation, Sci. Rep. 5 (2015) 18364.
[46] L. Cheng, J. Rui, Q. Li, H. Zhang, Y. Lu, Enrichment and dynamics of novel syntrophs in a methanogenic hexadecane-degrading culture from a Chinese oilfield, FEMS (Fed. Eur. Microbiol. Soc.) Microbiol. Ecol. 83 (3) (2013) 757–766.
[47] J. Cheng, J. Hua, T. Kang, B. Meng, L. Yue, H. Dong, H. Li, J. Zhou, Nanoscale zero-valent iron improved lactic acid degradation to produce methane through anaerobic digestion, Bioresour. Technol. 317 (2020) 124013.
[48] D.E. Ross, C.W. Marshall, D. Gulliver, H.D. May, R.S. Norman, Defining genomic and predicted metabolic features of the acetobacterium genus, mSystems 5 (5) (2020) e00277-00220.
[49] F. Bekhit, S. Farag, A.M. Attia, Characterization of immobilized magnetic Fe_3O_4 nanoparticles on *Raoultella ornithinolytica* sp. and its application for azo dye removal, Appl. Biochem. Biotechnol. 194 (12) (2022) 6068–6090.
[50] J.M.S. Oliveira, J.S. Poulsen, E. Foresti, J.L. Nielsen, Microbial communities and metabolic pathways involved in reductive decolorization of an azo dye in a two-stage AD system, Chemosphere 310 (2023) 136731.
[51] V. Chalansonnet, C. Mercier, S. Orenga, C. Gilbert, Identification of Enterococcus faecalis enzymes with azoreductases and/or nitroreductase activity, BMC Microbiol. 17 (1) (2017) 126.
[52] C. Van Steendam, I. Smets, S. Skerlos, L. Raskin, Improving anaerobic digestion via direct interspecies electron transfer requires development of suitable characterization methods, Curr. Opin. Biotechnol. 57 (2019) 183–190.
[53] T.T. An, F.W. Picardal, *Desulfuromonas carbonis* sp. nov., an Fe(III)-, S^0- and Mn(IV)-reducing bacterium isolated from an active coalbed methane gas well, Int. J. Syst. Evol. Microbiol. 65 (Pt 5) (2015) 1686–1693.
[54] T. Zhang, T.S. Bain, M.A. Barlett, S.A. Dar, O.L. Snoeyenbos-West, K.P. Nevin, D.R. Lovley, Sulfur oxidation to sulfate coupled with electron transfer to electrodes by *Desulfuromonas* strain TZ1, Microbiology 160 (Pt 1) (2014) 123–129.
[55] A. El Houari, M. Ranchou Peyruse, A. Ranchou Peyruse, A. Dakdaki, M. Guignard, L. Idouhammou, R. Bennisse, R. Bouterfass, R. Guyoneaud, A.I. Qatibi, *Desulfobulbus oligotrophicus* sp. nov., a sulfate-reducing and propionate-oxidizing bacterium isolated from a municipal anaerobic sewage sludge digester, Int. J. Syst. Evol. Microbiol. 67 (2) (2017) 275–281.
[56] A. Hussain, J. Lee, H. Ren, H.S. Lee, Spatial distribution of biofilm conductivity in a *Geobacter* enriched anodic biofilm, Chem. Eng. J. 404 (2021) 126544.
[57] D. Ozuolmez, H. Na, M.A. Lever, K.U. Kjeldsen, B.B. Jorgensen, C.M. Plugge, Methanogenic archaea and sulfate reducing bacteria co-cultured on acetate: teamwork or coexistence? Front. Microbiol. 6 (2015) 492.
[58] Y. Li, L. Crouzet, W.J. Kelly, P. Reid, S.C. Leahy, G.T. Attwood, *Methanobrevibacter boviskoreani* JH1T growth on alcohols allows development of a high throughput bioassay to detect methanogen inhibition, Current Research in Microbial Sciences 4 (2023) 100189.
[59] S. Zheng, F. Liu, B. Wang, Y. Zhang, D.R. Lovley, Methanobacterium capable of direct interspecies electron transfer, Environ. Sci. Technol. 54 (23) (2020) 15347–15354.
[60] M.O. Yee, O.L. Snoeyenbos West, B. Thamdrup, L.D.M. Ottosen, A.E. Rotaru, Extracellular electron uptake by two Methanosarcina species, Front. Energy Res. 7 (2019) 29.
[61] M.H. Cui, T. Sangeetha, L. Gao, A.J. Wang, Efficient azo dye wastewater treatment in a hybrid anaerobic reactor with a built-in integrated bio-electrochemical system and an aerobic biofilm reactor: evaluation of the combined forms and reflux ratio, Bioresour. Technol. 292 (2019) 122001.
[62] J. Thiel, S. Spring, B.J. Tindall, C. Spröer, B. Bunk, E. Koeksoy, D.K. Ngugi, B. Schink, M. Pester, *Desulfolutivibrio sulfoxidireducens* gen. nov., sp. nov., isolated from a pyrite-forming enrichment culture and reclassification of *Desulfovibrio sulfodismutans* as *Desulfolutivibrio sulfodismutans* comb. nov, Syst. Appl. Microbiol. 43 (5) (2020) 126105.
[63] J. Chen, M.J. Wade, J. Dolfing, O.S. Soyer, Increasing sulfate levels show a differential impact on synthetic communities comprising different methanogens and a sulfate reducer, J. R. Soc. Interface 16 (154) (2019) 20190129.
[64] Z. Cetecioglu, J. Dolfing, J. Taylor, K.J. Purdy, O. Eyice, COD/sulfate ratio does not affect the methane yield and microbial diversity in anaerobic digesters, Water Res. 155 (2019) 444–454.
[65] S. Cheng, D. Xing, D.F. Call, B.E. Logan, Direct biological conversion of electrical current into methane by electromethanogenesis, Environ. Sci. Technol. 43 (10) (2009) 3953–3958.
[66] K. Amit, K. Krishna, L. Piet, L. Dónal, Does bioelectrochemical cell configuration and anode potential affect biofilm response? Biochem. Soc. Trans. 40 (6) (2012) 1308–1314.
[67] X. Liu, Q. Chen, D. Sun, Y. Wang, H. Dong, Y. Dang, D.E. Holmes, Applying potentials to conductive materials impairs High-loading anaerobic digestion performance by affecting direct interspecies electron transfer, Bioresour. Technol. 297 (2020) 122422.